Inferring Ice/Ocean Surface Roughness from Horizontal Current Measurements

M. G. McPhee
McPhee Research Company,
Naches, WA 98937

Turbulence measurements in the underice boundary layer from two Arctic drift stations are used to develop a method for estimating the small-scale roughness, z_o, of the ice underside from horizontal current and current variance, sampled at one level. Horizontal variance is shown to be well correlated with turbulent kinetic energy (TKE). Measurements also indicate that at depths where turbulence is fully developed to the surface roughness, shear production of TKE is approximately in balance with viscous dissipation, so that the magnitude of local horizontal stress is proportional to flow variance. A similarity model is used to extrapolate local stress to the interface, and z_o is estimated from the logarithmic profile for current speed. The method has application for using remote data buoys, equipped with "smart" current meters, for mapping the underice roughness.

1 Background

Theoretical treatments of sea ice dynamics tend to emphasize the constitutive relation between internal ice stress and macroscale strain of the ice pack (e.g., Hibler, 1979), but data from drifting buoys and manned stations indicate that most of the time, drift of pack ice is controlled by air and water stress at the upper and lower horizontal boundaries. Thorndike and Colony (1982) estimated correlation coefficients between geostrophic wind and ice drift as 0.95 for summer and 0.85 for winter, for ice away from the immediate influence of coastlines. Their observations do not preclude internal ice stress gradients, but the high correlation between wind and drift indicates that internal stress is rarely more important than water stress in the force balance. During summer, internal stress gradients are often practically negligible in the force balance (McPhee, 1979). It can thus be argued that for understanding ice motion, the boundary-layer constitutive law governing stress at the ice/ocean interface is at least as important as the material stress-strain relation, and that as our models, data base, and operational requirements become better developed, relegating all the physics of ice/ocean momentum transfer to a standard drag coefficient will prove inadequate.

Several factors affect the oceanic drag on sea ice. Under certain conditions, buoyancy modifies momentum transfer either by changing the turbulence structure (Mellor et al., 1986) or by internal wave drag (Morison et al., 1987), but overall, the most important factor determining ice velocity relative to the underlying ocean is the topographic relief of the ice undersurface. The hydraulic roughness manifests itself both in the smaller scale roughness length, z_o, responsible for generating turbulent "skin friction," and as a larger scale distribution of pressure ridge keels which exert a "form drag" force analogous to mountain drag in the atmosphere. The partition of total drag between the two types of roughness is not well understood. By considering local turbulence measurements compared with total Ekman transport in the boundary layer, McPhee and Smith (1976) estimated that skin friction and keel form drag contributed about equally to the total drag during AIDJEX 72 in the Beaufort Sea. On the other hand, McPhee et al. (1987) found that skin friction, at least as indicated by local turbulence 4 m below the ice/ocean interface, roughly balanced wind stress, thus accounting for most of the oceanic drag.

Recent studies of turbulent stress in the underice boundary layer have shown that the small scale roughness, z_o is highly variable. Consider the comparison of ice/ocean traction vectors shown in Fig. 1. Each stress was calculated from a so-called "Rossby similarity" drag law—the equivalent for rotating planetary boundary layers, of the better known "law of the wall" for logarithmic surface layers; see McPhee (1986a)—using a fixed velocity of 20 cm/s, and surface roughness length, z_o, determined from actual turbulence measurements in the underice boundary layer at three different locations: MIZEX (Marginal Ice Zone Experiment, Greenland Sea, July 1984); AIWEX (Arctic Internal Wave Experiment, Beaufort Sea, April 1985); and the ARAMP (Arctic Remote Autonomous Measurement Platform) test in the Beaufort Sea, March 1987. In all three cases, data were obtained with the same instrumentation and reduced in the same way. To understand ice/ocean momentum flux, we need to know why z_o varies in space and time, and how much of the variation is compensated by adjustment in larger scale form drag.

In the past, turbulence measurements have been limited to manned drift stations, which require major logistics support. Modern data buoys offer wider coverage for longer times, and

Contributed by the OMAE Division and presented at the 7th International Symposium and Exhibit on Offshore Mechanics and Arctic Engineering, Houston, Texas, February 7–12, 1988, of THE AMERICAN SOCIETY OF MECHANICAL ENGINEERS. Manuscript received by the OMAE Division, 1987; revised manuscript received October 7, 1988.

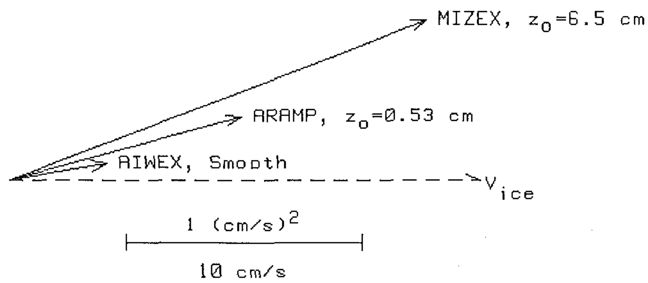

Fig. 1 Variation in ice/water stress for various roughness lengths found in recent projects, for constant ice velocity of 20 cm/s. Stress is calculated from a Rossby similarity law.

are relatively much less expensive than manned camps. The intent of this paper is to show that measurements made with a single commerically available, "smart" current meter, suspended in the boundary layer under unmanned data buoys, can in principle, be used to estimate the underice roughness with reasonable confidence. To show this, we use Reynolds stress and turbulent kinetic energy data, measured with special turbulence clusters during two recent manned drift experiments in the Arctic (MIZEX 1984 and the 1987 ARAMP test). A method is developed for estimating z_o (including confidence limits) from horizontal mean current and current variance at one level in the boundary layer.

2 Turbulence Data

Three-dimensional turbulence data from two projects (MIZEX 84 and the 1987 ARAMP test) are used in this section to show: 1) turbulent kinetic energy of flow in the upper few meters of the underice PBL is well estimated by the two horizontal variance components in the Reynolds stress tensor; and 2) for measurements far enough from the interface, shear production of turbulent kinetic energy is approximately balanced by viscous dissipation, so that the horizontal component of local turbulent Reynolds stress can be estimated from the total variance. Given local stress at a particular level, we can extrapolate stress to the interface using a simple similarity model for PBL stress attenuation with depth, and deduce z_o from the mean velocity at the measurement level.

Instrumentation used to measure turbulence comprises clusters of 4-cm-dia, partially ducted current meters mounted along three orthogonal axes in a horizontal plane, near fast response temperature and conductivity meters. In MIZEX 84, clusters were mounted at 6 levels on inverted masts in the underice PBL at depths ranging from 1 to 15 m below the interface. One cluster was mounted 2 m below the ice at a remote location about 100 m from the main mast. In ARAMP, clusters were mounted at 2, 4, and 5 m below the interface. Configuration and calibration of the measurement system is described by McPhee (1986b), with some results for the MIZEX 1984 project in the Greenland Sea marginal ice zone presented by McPhee et al. (1987) and Morison et al. (1987).

There are a number of contrasts between the boundary layers measured during summer at MIZEX 84 and near the end of winter at ARAMP. Surface roughness at MIZEX was an order of magnitude larger than at ARAMP (Fig. 1). The mixed layer was shallow (10–20 m) with small, but persistent positive buoyancy from surface melt at MIZEX, while at ARAMP it was well mixed (neutrally stable) to about 30 m. Inertial oscillations were energetic at MIZEX, but nearly absent at ARAMP. Overall, the flow regimes were quite different, and we presume that any similarities in turbulence at the two sites would be of a fairly general nature.

2.1 Turbulence Statistics. By applying the Reynolds averaging technique to the fluid equations, and assuming a spectral gap between wave numbers characterizing the energy containing turbulent eddies and other fluctuations in the flow, it can be shown (see, e.g., Tennekes and Lumley, 1972) that inertial forces associated with turbulent overturn can be represented by the gradient of a symmetric stress tensor with components

$$\begin{vmatrix} \langle u'u' \rangle & \langle u'v' \rangle & \langle u'w' \rangle \\ \langle u'v' \rangle & \langle v'v' \rangle & \langle v'w' \rangle \\ \langle u'w' \rangle & \langle v'w' \rangle & \langle w'w' \rangle \end{vmatrix}$$

where, e.g., $u' = u - \langle u \rangle$, u is the instantaneous component of flow along the x-axis, and $\langle\ \rangle$ denotes ensemble averaging.

In this work, we are concerned with the horizontal component of Reynolds stress, scalar magnitude of which is characterized by the local friction velocity

$$u_* = \{\langle u'w' \rangle^2 + \langle v'w' \rangle^2\}^{1/4}$$

and two measures of flow variance, which we also characterize by velocity scales

$$q = \{\langle u'u' \rangle + \langle v'v' \rangle + \langle w'w' \rangle\}^{1/2}$$

$$q_h = \{\langle u'u' \rangle + \langle v'v' \rangle\}^{1/2}$$

Note that half-q^2 is the turbulent kinetic energy (TKE) per unit mass of the flow, and also that our definition of u_* refers to the local stress velocity scale. The special notation, u_{*o}, refers to the friction velocity at the interface.

The ensemble average is estimated by dividing the time series of flow at one location into separate realizations assuming that spatial variation is advected past the probe with the mean flow. Turbulent statistics are calculated for each realization, with mean vector and tensor quantities rotated into a coordinate system with w (z-axis) vertical. Care is required in the choice of the averaging interval; we found from numerous tests that 15 min fell about midway in the so-called spectral gap between the time scale of the largest turbulent eddies and the scale at which larger, nonturbulent fluctuations began to affect the covariance tensor. It should be noted that the time scale of the largest eddies, typically 3–6 min, is a sizable portion of the averaging interval, so that one expects much variability in flow statistics from one realization to the next.

Data from both projects were assembled and analyzed in 15-min realizations, and edited to include only segments for which the mean speed and separate components exceeded threshold limits of 5 cm/s and 2 cm/s, respectively. Data from the last nine days of MIZEX were excluded, because of rapid melt and stratification. Scatter plots and regression lines for q_h versus q are shown for each project in Fig. 2. These include all 15-min samples for each cluster except the one at 15 m in MIZEX, which was often in stratified fluid below the mixed layer. The similarity is striking, and indicates that horizontal variance can be used to predict turbulent kinetic energy with reasonable certainty.

Relating u_* to q is less obvious. There is guidance from laboratory and atmospheric boundary layers where shear production of TKE is equal to viscous dissipation. Mellor and Yamada (1982, Table 1) summarized a number of studies where production balanced dissipation and found the average ratio, q/u_*, to be 2.55, but with considerable scatter. Under sea ice, the turbulent flow is complicated by local pressure gradients associated with underice topography. McPhee and Smith (1976) showed that during AIDJEX 72, the profile of downstream Reynolds stress was distorted by local pressure gradients, and inferred that near the surface dissipation was about twice shear production. McPhee et al. (1987) found that Reynolds stress increased from 1 to 4 m at MIZEX, and suggested that at depths less than 4 m, the turbulence was not fully developed to the actual roughness representative of the

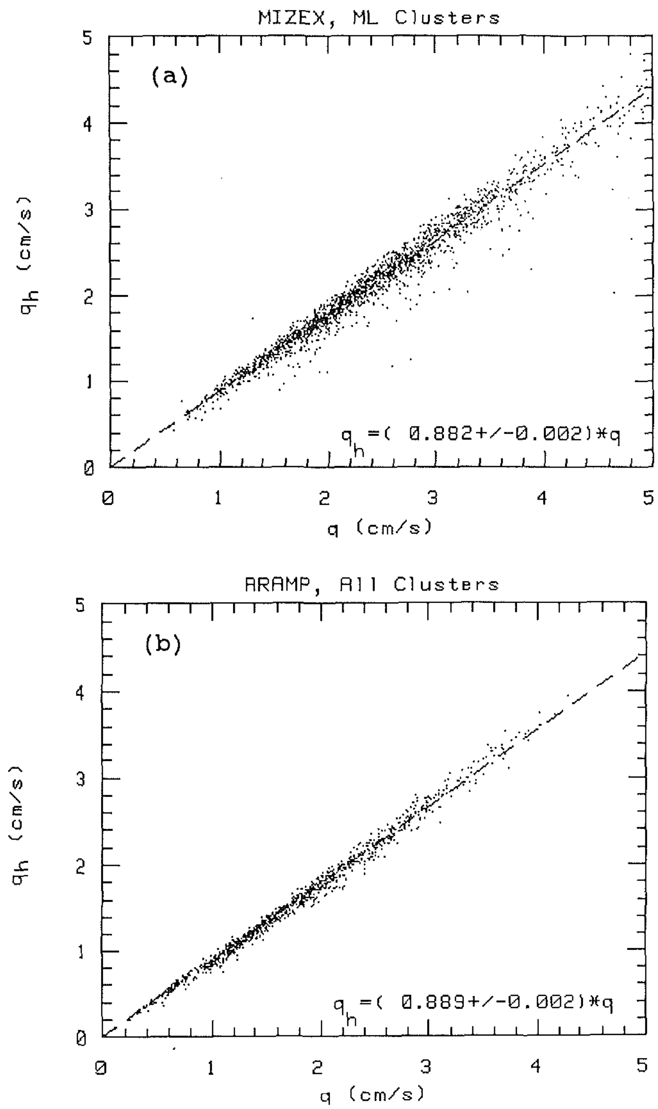

Fig. 2 Square root of horizontal variance versus square root of total variance for mixed-layer clusters in MIZEX 84 (*a*) and all clusters in ARAMP (*b*). Regression slope with 95 percent confidence limits is listed.

floe. A numerical model forced by observed wind stress at the MIZEX site showed stress decreasing monotonically from the interface, and matched observed stress quite closely at the 4-m level. A similar result was found at the ARAMP test site (McPhee, unpublished report, 1987), which was approximately 25 m upstream from a small pressure ridge keel. At ARAMP the stress at 5 m was about twice as large as at 2 m, and there was a fairly large increase from 4 to 5 m. We again inferred that measurements had to be several meters away from the interface before turbulent stress was representative of the larger area controlling the entire boundary layer structure. Scatter diagrams and regression lines of q versus u_* at 4 m during MIZEX and 5 m during ARAMP are shown in Fig. 3. Note that the slopes bracket the average value (2.55) used by Mellor and Yamada (1982). Regression slopes with 95 percent confidence limits for all clusters are listed in Table 1. In both cases, there is an increase close to the interface, which implies that in locally smooth areas, shear production cannot account for the levels of turbulence observed. An important implication is that for measurements near the interface, flow variance may often be a better indicator of average turbulent stress than the actual measured Reynolds stress. In any case, flow variance is the only turbulence measurement possible with a two-component current meter, so we follow Mellor and Yamada (1982), and estimate local friction velocity as $u_* = q/2.55$.

2.2 Friction Velocity and Surface Roughness. In atmospheric studies, stress measuring instruments are usually deployed in the so-called surface layer. This allows two important simplications: 1) stress in the surface layer is assumed constant, and 2) wind (analogous to current measured with respect to the drifting ice) and stress are assumed collinear. Tennekes (1973) suggests that the outer limit for the surface layer in neutral stability is $0.03u_{*o}/f$ (f is the Coriolis parameter), which is typically about 2 m in the underice PBL. For reasons discussed in the last subsection, it is often desirable to deploy instruments several meters below the interface, where stress is attenuated by rotational effects relative to the actual interfacial stress. The following expression for determining u_{*o} from u_* at the measurement level is based on the analytic similarity PBL model of McPhee (1981, see equation (16)).

$$u_{*o} = u_* \exp\{f|z|\gamma_R/(2u_{*o})\} \tag{1}$$

Table 1 Ratio q_h/q and q/u_* with 95 percent confidence limits for all mixed-layer clusters, both projects

MIZEX (Greenland Sea, July, 1984)

Cluster	Depth (m)	q_h/q	q/u_*
1	1	0.924 ± 0.004	2.96 ± 0.08
2	2	0.884 ± 0.004	2.61 ± 0.05
3	4	0.873 ± 0.004	2.44 ± 0.05
4	7	0.877 ± 0.006	2.34 ± 0.04
6 (Rem)	2	0.903 ± 0.003	2.50 ± 0.04

ARAMP (Beaufort Sea, March, 1987)

Cluster	Depth (m)	q_h/q	q/u_*
1	2	0.903 ± 0.003	3.14 ± 0.07
2	4	0.887 ± 0.003	3.01 ± 0.07
3	5	0.887 ± 0.003	2.62 ± 0.06

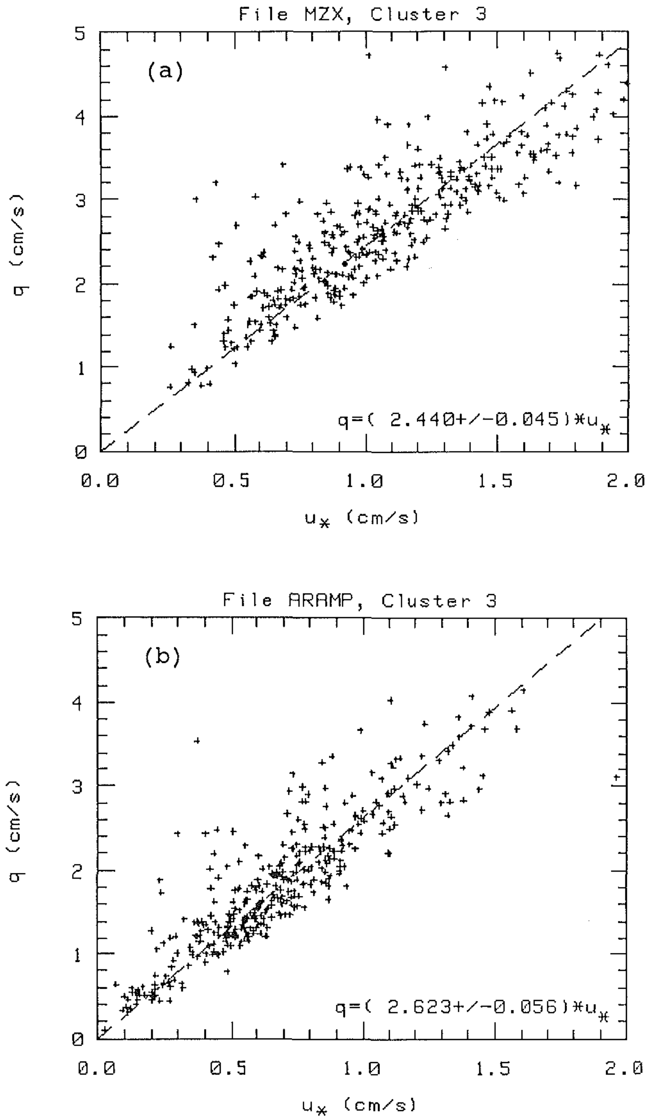

Fig. 3 q versus u* (local) for cluster at 4 m in MIZEX 84 (*a*) and 5 m in ARAMP (*b*). Regression slope with 95 percent confidence limits is listed.

where $\gamma_R = 4.9$ is a nondimensional constant derived from the vertical length scale of energy-containing eddies in the turbulent flow. For specified u_* and z, (1) is easily solved by iteration.

Given u_*, the effective surface roughness is found from mean velocity at the measurement level, which is generally outside of the surface layer. If the measurement distance is several times the surface layer thickness, then z_o and the angle between interfacial stress and measured velocity should be determined using the similarity solutions described in McPhee (1981). On the other hand, if measurements are made within two or three times the maximum surface layer extent, the logarithmic profile closely approximates the similarity solution, and stress is in the direction of relative velocity. In that case,

$$\ln z_o = \ln |z_m| - kU(z_m)/u_{*o} \qquad (2)$$

where $k = 0.4$ is von Karman's constant.

Note that $\ln z_o$ is a linear function of U/u_{*o}, not U/u_* as it would be if stress were constant. The development here assumes neutral stability, i.e., that ice melt or growth is not excessive, and that the mixed layer extends well past the measurement level. Where buoyancy becomes a major factor in the PBL physics, the similarity methods (McPhee, 1981) may be used instead, but then transient effects are likely to contaminate the results at any rate.

We used the turbulence clusters to simulate fast sampling current meters with two horizontal axes, and calculated u_{*o} from the horizontal variances for each 15-min segment, using (1) with $u_* = q_h/\{(0.88)(2.55)\}$. Regression slopes with 95 percent confidence limits for all clusters are listed in Table 2.

We also calculated $\ln z_o$ for each 15-min segment and determined mean and variance of $\ln z_o$ at each cluster level. Results are listed in Table 2, along with the 95 percent confidence interval for z_o. Note that the effective z_o increases with measurement depth, except between 4 and 7 m at MIZEX, where confidence limits overlap. This is consistent with the idea that turbulence levels near a smooth surface do not necessarily reflect the fully developed turbulence of the entire boundary layer.

Frequency histograms of $\ln z_o$ for clusters considered to be in the fully developed turbulence regions, i.e., 7 m at MIZEX and 5 m at ARAMP, are shown in Fig. 4, along with Gaussian (normal) probability distribution functions based on the

Table 2 u_{*o}/U ratios with 95 percent confidence limits for all mixed-layer clusters, both projects, along with mean and variance of $\ln z_o$. Last column is the range of z_o implied by 95 percent confidence interval for $\ln z_o$.

MIZEX (Greenland Sea, July, 1984)

Cluster	Depth (m)	u_{*o}/U	$<\ln z_o>$	Variance	z_o range (cm)
1	1	0.085 ± 0.004	-4.57	2.56	0.87 to 1.25
2	2	0.094 ± 0.004	-3.42	2.70	2.76 to 3.88
3	4	0.095 ± 0.004	-2.73	2.81	5.50 to 7.73
4	7	0.080 ± 0.003	-3.05	2.72	4.04 to 5.56
6 (Rem)	2	0.071 ± 0.002	-4.96	3.05	0.59 to 0.84

ARAMP (Beaufort Sea, March, 1987)

Cluster	Depth (m)	u_{*o}/U	$<\ln z_o>$	Variance	z_o range (cm)
1	2	0.056 ± 0.001	-6.68	3.42	0.10 to 0.15
2	4	0.057 ± 0.001	-5.89	3.45	0.23 to 0.33
3	5	0.060 ± 0.001	-5.24	2.76	0.45 to 0.63

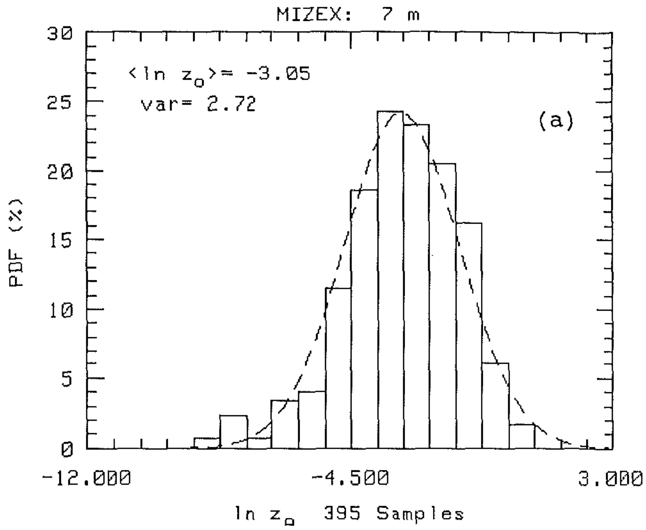

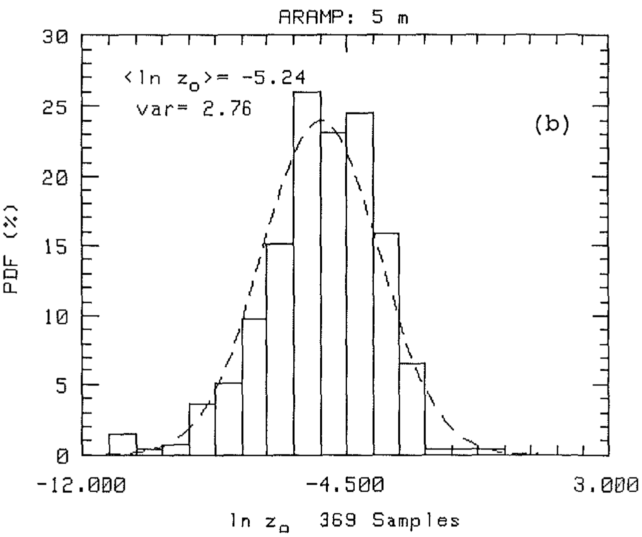

Fig. 4 Histograms of ln z_o and Gaussian probability distribution functions from listed mean and variance for MIZEX cluster at 7 m (*a*), and ARAMP cluster at 5 m (*b*)

measured mean and variance. Two significant results are apparent: first, the PDF implied by the histograms appears to be approximately normal, and second, the standard deviations are quite similar for MIZEX and ARAMP, despite large difference in mean roughness. Under assumptions of normality and known standard deviation (the average is 1.66), we can assign confidence limits to estimates of z_o drawn from limited numbers of (15-min) samples. This information should aid in design of sampling strategies for remote buoys, which have to be as power conservative as possible. Suppose, for example, we wish to know the minimum sampling time for determining z_o at some location to within a factor of 1.5. Stated more formally, if $\langle z_o \rangle$ is the average of 15-min samples used to estimate z_o, what is the minimum number of samples, n, required such that the interval $\langle z_o \rangle/1.5$ to $1.5\langle z_o \rangle$ contains z_o 95 percent of the time? The confidence limits are $\ln(1.5) = 1.96\sigma/\sqrt{n}$. For $\sigma = 1.66$, $n = 64$, i.e., 16 hr of data.

3 Summary

Data from extensive measurements of three-dimensional turbulence in the ice/ocean boundary layer have been used to develop a method for estimating interfacial stress and small-scale roughness, z_o, from horizontal current and current variance measured at one level. The method assumes that shear production of turbulent kinetic energy is balanced by viscous dissipation, so that local turbulent stress is proportional to TKE, which is estimated from the horizontal variance. The measurement level should be deep enough in the boundary layer for the turbulence to be fully developed, which often requires that the local stress be adjusted for estimating interfacial stress. The logarithmic profile for mean velocity is assumed to hold for up to 2 or 3 times the surface layer thickness, but this requirement may be relaxed if, e.g., the similarity theory of McPhee (1981) is used.

Statistics of $\ln(z_o)$ calculated by the method for two projects with different roughness and PBL characteristics indicates that the standard deviation of $\ln(z_o)$ estimates is constant, about 1.66. This number can be used for estimating confidence intervals, and sample requirements.

The method provides a means of using unmanned data buoys to greatly increase our sampling of small-scale, underice hydraulic roughness in both space and time.

Acknowledgment

Logistics support from the Polar Science Center, University of Washington, and field assistance from WHOI/MIT scientists in the ARAMP development program is much appreciated. This work was funded by the Office of Naval Research under Contract N00014-84-C-0028.

References

Hibler, W. D., III, 1979, "A Dynamic Thermodynamic Sea Ice Model," *Journal of Physical Oceanography*, Vol. 9, pp. 815–846.

McPhee, M. G., 1979, "The Effect of the Oceanic Boundary Layer on the Mean Drift of Pack Ice: Application of Simple Model," *Journal of Physical Oceanography*, Vol. 9, pp. 388–400.

McPhee, M. G., 1981, "An Analytic Similarity Theory for the Planetary Boundary Layer Stabilized by Surface Buoyancy," *Boundary-Layer Meteorology*, Vol. 21, pp. 325–339.

McPhee, M. G., 1986a, "The Upper Ocean," *The Geophysics of Sea Ice*, ed., N. Untersteiner, Plenum, New York, pp. 339–394.

McPhee, M. G., 1986b, "A Velocity/Temperature/Conductivity Measuring System for the Underice Environment," *Proceedings of the IEEE Third Working Conference on Current Measurement*, eds., G. F. Appell and W. E. Woodward, Institute of Electrical and Electronics Engineers, New York, pp. 215–220.

McPhee, M. G., Maykut, G., and Morison, J. H., 1987, "Dynamics and Thermodynamics of the Ice/Upper Ocean System of the Marginal Ice Zone of the Greenland Sea," *Journal of Geophysical Research*, Vol. 92, pp. 7017–7031.

McPhee, M. G., and Smith, J. D., 1976, "Measurements of the Turbulent Boundary Layer Pack Ice," *Journal of Physical Oceanography*, Vol. 6, pp. 696–711.

Mellor, G. L., McPhee, M. G., and Steele, M., 1986, "Ice-Seawater Turbulent Boundary Layer Interaction With Melting on Freezing," *Journal of Physical Oceanography*, Vol. 16, pp. 1829–1846.

Mellor, G. L., and Yamada, T., 1982, "Development of a Turbulence Closure Model for Geophysical Fluid Problems," *Review of Geophysics and Space Physics*, Vol. 20, pp. 851–875.

Morison, J. H., McPhee, M. G., and Maykut, G., 1987, "Boundary Layer, Upper Ocean, and Ice Observations in the Greenland Sea Marginal Ice Zone," *Journal of Geophysical Research*, Vol. 92, pp. 6987–7011.

Tennekes, H., 1973, "The Logarithmic Wind Profile," *Journal of Atmospheric Science*, Vol. 30, pp. 234–239.

Tennekes, H., and Lumley, J. L., 1972, *A First Course in Turbulence*, The MIT Press, Cambridge, Mass.

Thorndike, A. S., and Colony, R., 1982, "Sea Ice Motion in Response to Geostrophic Winds," *Journal of Geophysical Research*, Vol. 87, pp. 5845–5852.